ACADEMIC PRESS

Available online at www.sciencedirect.com

SCIENCE DIRECT®

Journal of Structural Biology 143 (2003) 1–13

Journal of Structural Biology

www.elsevier.com/locate/yjsbi

# Anti-cementoblastoma-derived protein antibody partially inhibits mineralization on a cementoblastic cell line

Marco Antonio Alvarez Pérez,[a] Sandu Pitaru,[b] Octavio Alvarez Fregoso,[c] José Reyes Gasga,[d] and Higinio Arzate[a,*]

[a] *Laboratorio de Biología Celular y Molecular, Facultad de Odontología, UNAM, Mexico*
[b] *The Maurice and Gabriela Goldschleger, School of Dental Medicine, Tel Aviv University, Israel*
[c] *Instituto de Investigación en Materiales, UNAM, Mexico*
[d] *Instituto de Física, UNAM, Mexico*

Received 23 October 2002, and in revised form 30 April 2003

**Abstract**

The effect of human anti-cementoblastoma-derived protein antibody during cementogenesis in vitro was investigated by using human cementoblastoma-derived cells. Cultures treated with 5 μg/ml of CP antibody from day 1 to day 15 revealed a significant decrease in alkaline phosphatase activity (ALP) 40% ($p < 0.005$), 44% ($p < 0.001$), 49% ($p < 0.1$), and 45% ($p < 0.02$) at 9, 11, 13, and 15 days, respectively. Immunoexpression of osteopontin revealed that in cultures treated with anti-CP antibody, the positive number of cementoblastoma cells was reduced by 87, 83, 69, and 52% at 5, 7, 9, and 11 days, respectively. Bone sialoprotein immunoexpression showed a decrease in positive cells of 82, 51, 60, 80, 83, and 87% at 5, 7, 9, 11, 13, and 15 days, respectively, as compared to controls. The Ca/P ratio of the mineral-like tissue deposited in vitro by cementoblastoma cells revealed that control cultures had a Ca/P ratio of 1.45 and 1.61 at 5 and 15 days, whereas experimental cultures revealed a Ca/P ratio of 0.50 and 0.79 at 5 and 15 days, respectively. Electron diffraction patterns showed inner double rings representing D-spacing that were consistent with those of hydroxyapatite in both control and experimental cultures. Examination of the crystallinity with high resolution transmission electron microscopy showed homogeneous and preferential spatial arrangement of hydroxyapatite crystallites in control and experimental cultures at 15 days. Atomic force microscopy images of control cultures at 5 and 15 days revealed small granular particles and grain agglomeration that favored the formation of crystalline plaques with a lamellar-like pattern of the mineral-like tissue. Experimental cultures at 5 and 15 days showed tiny and homogeneous granular morphology. The agglomerates maintained spherical morphology without organization of needle-like crystals to form plaque-like structures. Based on these findings, it is hypothesized that cementoblastoma-derived protein may be associated to crystal growth, compositional and morphological features during the mineralization process of cementum in vitro.


*Keywords:* Cementum; Cementoblastoma-derived protein; Bone sialoprotein; Hydroxyapatite; Mineralization; Osteopontin

## 1. Introduction

Cementum is a unique avascular mineralized connective tissue that surrounds the root dentine and provides the interface through which the root surface is anchored to the collagen Sharpey's fibers of the periodontal ligament. Cementum matrix consists of collagen types I and III, fibronectin, osteopontin (OPN), bone sialoprotein (BSP) (Bosshardt et al., 1998; Nanci, 1999), and osteocalcin (OCN) (D'Errico et al., 2000; Kagayama et al., 1997; MacNeil et al., 1998).

OPN and BSP have been implicated in mineral deposition and cell– and matrix–matrix interactions (Boskey, 1995). These proteins have been proposed to be potential regulators of the hydroxyapatite crystal nucleation and/or growth. OPN has a poly-Asp and BSP two poly-Glu domains, whose repetitive sequences are known to bind calcium to mineral surfaces. OPN is a highly phosphorylated and sulfated sialoprotein with an

* Corresponding author. Fax: +52(55)56225563.
*E-mail address:* harzate@servidor.unam.mx (H. Arzate).

1047-8477/$ - see front matter © 2003 Elsevier Science (USA). All rights reserved.
doi:10.1016/S1047-8477(03)00116-3

RGD motif attachment that recognizes the vitronectin type of the integrin receptor. Periodontium cells in close contact with acellular cementum and cellular cementum, express OPN as well as cementocytes (Bronckers et al., 1994).

BSP is also an RGD-containing sialoprotein with cell attachment properties (Oldberg et al., 1988). It has been suggested that it is involved in controlling the formation and resorption of mineralized tissues as well as in the nucleation of hydroxyapatite crystals at the mineralizing front of bone (Chen et al., 1992a). BSP is believed to play a critical regulatory role during the process of cementogenesis and this molecule might be involved in the processes of precementoblast chemoattraction, adhesion, and differentiation (MacNeil et al., 1995).

Recent studies suggest that cementum may contain unique molecules that are specific for this tissue (McAllister et al., 1990). The cementum attachment protein (CAP) has been characterized as a collagenous protein with an $M_r$ of 56 000 (Wu et al., 1996), and its location appears to be restricted to cementum (Arzate et al., 1992). This molecule has been shown to promote adhesion and spreading of mesenchymal cell types (Olson et al., 1991), and alkaline phosphatase expression and mineralization in undifferentiated mesenchymal cells (Arzate et al., 1996). CAP promotes selectively the attachment of mineralized tissue forming periodontium lineages (Pitaru et al., 1995), serves as a marker for putative cementoblastic progenitors of the adult human periodontal ligament (Bar-Kana et al., 1999; Liu et al., 1997), and affects the differentiation of these progenitors in vitro (Saito et al., 2001).

Recently, we isolated and characterized a human cementoblastoma-derived cell line that expresses the cementum phenotype. The physical, morphological and chemical features of the cementum-like tissue deposited by these cells appeared to be different from the mineral-like tissue deposited by human osteoblastic cells in vitro, and is similar to human cellular cementum (Arzate et al., 1998, 2000). This cell line produces a cementum protein species of 56 kDa that has been purified from its conditioned media. The cementoblastoma-derived protein (CP) promotes attachment on human gingival fibroblasts, human periodontal ligament cells, and alveolar bone-derived cells in a dose-dependent manner. CP has also been postulated to be related to CAP since a monoclonal antibody against bovine CAP cross-reacted with immunopurified CP as a 70 kDa species (Arzate et al., 2002). A polyclonal antibody raised against CP revealed that CP is widely distributed throughout cementum and is able to identify putative cementoblastic populations both in vivo and in vitro (Arzate et al., 2002). Thus, the antibody raised against CP could serve as an in vitro model to study the mineralization process in this characterized cementoblastic cell line.

## 2. Materials and methods

Rabbit polyclonal antiserum to human OPN (LF-123), and human BSP (LF-100) were kindly donated by Dr. Larry Fisher from NIH.

### 2.1. Antibody preparation

CP's partial purification was performed as described by McAllister et al. (1990). Three liters of conditioning media obtained from human cementoblastoma-derived cells were dialyzed against PBS and lyophilized, then reconstituted in PBS and loaded into a DEAE-cellulose column. The 0.5 M NaCl fraction was loaded on SDS–PAGE gel and the CP band with an $M_r$ of 56 000 was excised from the gel. Gel slices were electroeluted in 50 mM $NH_4HCO_3$ containing 0.1% SDS. SDS was removed by extracting with acetone at −20 °C and lyophilized. New Zealand rabbits were immunized through subcutaneous (s.c.) injections with a 5-μg dose of CP mixed with $Al(OH)_3$ (v/v), in the muscle of the right hind leg every two weeks for two months (Dunbar and Schwoebel, 1990). Seven days after the last immunization, the rabbits were bled, sera pooled, and frozen. Antibody production was monitored by ELISA and Western blot. Antiserum was purified through protein A–Sepharose chromatography. Antibodies bound to Protein A were washed with PBS and eluted with a solution of 0.2 M glycine–HCl, pH 2.6. Eluted antibodies were immediately neutralized with 10× PBS, and dialyzed against PBS. The specificity of the anti-CP antibody was tested by immunoblotting and immunostaining as described previously in detail (Arzate et al., 2002). The antibody fraction will be referred to as anti-CP antibody.

### 2.2. Cell culture and anti-CP treatment

Cell cultures were derived from a human cementoblastoma, a neoplasm accepted as being essentially cementogenic by the World Health Organization (Kramer et al., 1992), through the conventional explant technique; cells were characterized as previously described (Arzate et al., 1998, 2000). Cementoblastoma cells were cultured in 75 $cm^2$ cell culture flasks containing DMEM, supplemented with 10% FBS and antibiotic solution (100 μg/ml streptomycin and 100 U/ml penicillin, Sigma Chemical). The cells were incubated in a 100% humidified environment at 37 °C in a 95% air and 5% $CO_2$ atmosphere. Human cementoblastoma-derived cells at the second passage were used for all the experimental procedures.

### 2.3. Proliferation assay

To determine whether IgG or anti-CP antibodies affected cell proliferation, human cementoblastoma-de-

rived cells were plated at $2 \times 10^4$ into 48-well culture plates and incubated overnight in 10% FBS. The following day, designated as day 0, the medium was changed and cultures were treated with 10% FBS plus anti-CP antibody (5 μg/ml). Control cultures were treated with a normal rabbit IgG antibody (5 μg/ml). Medium and antibodies were changed every other day. Cells were harvested by trypsinization (0.05% trypsin and 0.02% EDTA) and counted in a model ZBI Coulter Counter (Coulter Electronics, Hialeah, FL). Cell numbers were assessed at days 1, 3, 5, and 10. Experiments were performed in triplicate and repeated twice.

### 2.4. Cell viability assay

Cementoblastoma-derived cells viability in the presence of anti-CP antibodies was determined through the MTT assay. This assay is based on the ability of mitochondrial dehydrogenases to oxidize thiazolyl blue (MTT), a tetrazolium salt (3-[4,5-dimethylthiazolyl-2-y]-2,5-diphenyltetrazolium bromide), to an insoluble blue formazan product. Cells were plated at $1 \times 10^4$ into a 96-well plate by triplicate and incubated for 1, 3, 5, and 10 days. After each term, cells were incubated with MTT (120 mg/ml) at 37 °C for 3 h. After the supernatant was removed, 0.04 M HCl in isopropanol was added to each well and the optical density of the solution was read at 570 nm in an enzyme-linked immunoassay (ELISA) plate reader. Since generation of the blue product is proportional to the dehydrogenase activity, a decrease in absorbance at 570 nm provides a direct measurement of the number of viable cells. Experimental cultures were treated with 5 μg/ml of anti-CP antibody. Controls were treated with 5 μg/ml of IgG antibody. Experiments were performed in triplicate and repeated separately twice.

To test the effect of anti-CP antibodies on the mineral tissue formation, human cementoblastoma-derived cells were cultured for 5, 7, 9, 11, 13, and 15 days in DMEM supplemented as described above. Immediately after plating the cells and every other day, experimental cultures were treated with anti-CP antibody (5 μg/ml) and control cultures were treated with normal rabbit IgG antibodies (5 μg/ml) as described by Shakibaei (1998). At each time point cultures were tested for alkaline phosphatase activity and expression of OPN and BSP as described below.

### 2.5. Alkaline phosphatase activity

Human cementoblastoma-derived cells were plated in triplicate at $2 \times 10^4$ in 24-well culture plates (Costar, Cambridge MA, USA). Cells were cultured in DMEM, supplemented with 10% FBS, antibiotic solution, 10 mM β-glycerophosphate, 50 μg/ml ascorbic acid, and $10^{-7}$ M dexamethasone. Control and experimental cultures were treated as described above immediately after platting the cells. Fresh medium and antibody were added to the cultures every other day. Alkaline phosphatase activity (ALP) was determined according to Lowry et al. (1954). Cell layers were extracted in 10 mM Tris–HCl buffer, pH 7.4, containing 0.1% Triton X-100 and then sonicated. Enzyme activity was assessed using 8 mM disodium *p*-nitrophenyl phosphate (PNP) as the substrate and 2 mM $MgCl_2$ in 0.1 M Tris–HCl buffer, pH 9.8, and incubated at 37 °C for 30 min. The reaction was stopped by adding 50 μl of 0.05 N NaOH and absorbances were measured at 405 nm. Samples were assayed under conditions that ensured linearity with respect to time and protein concentrations. Protein concentrations were determined according to the Bradford (1976) assay using BSA as standard. Assays were repeated at least three times.

### 2.6. Immunofluorescence

Human cementoblastoma-derived cells were plated at low density ($5 \times 10^2$) in 8-well Lab-Tek chamber slides; allowed to attach overnight and cultured for the time periods mentioned above. At each term, cells were then fixed in 3.7% formaldehyde, and screened for the expression of BSP and OPN. Slides were incubated with anti-human OPN (LF-123) and anti-human BSP (LF-100), diluted 1:300 in PBS containing 1 mg/ml BSA and incubated overnight at 4 °C. Slides were washed with ice-cold phosphate-buffered saline (PBS) for 10 min at room temperature and incubated for 1 h at 4 °C with the secondary antibody goat-anti-rabbit immunoglobulin conjugated with FITC (3 mg/ml, Sigma Chemical, St. Louis, MO), diluted 1:50 in PBS. Slides were rinsed with PBS plus 0.1% Triton X-20 and coverslipped in glycerol–PBS (1:9 v/v) containing 20 mg/ml of 1,2,diazabycyclo (2.2.2) octane (DABCO; triethylenediamine). Immunostaining was visualized by indirect immunofluorescence (Axiophot, Carl Zeiss).

The number of cells cross-reacting with anti-OPN and anti-BSP was determined by scoring five different microscopic fields with a 20× lens. Results are expressed as means $(n = 5) \pm \mathrm{SE}$ of three independent experiments. Slides incubated with pre-immune rabbit serum or lacking first antibody were used as negative controls.

### 2.7. Western blot analysis

The relative levels of OPN and BSP of cementoblastoma cells treated with anti-CP antibody were compared with those treated with IgG antibody. Cementoblastoma-derived cells were plated in triplicate at $5 \times 10^4$ density on 35 mm culture dishes. Experimental and control cultures were treated as described above and cultured during 5, 7, 9, 11, 13, and 15 days. At each term, cells were scraped with a policeman, re-suspended with ice-cold PBS, and centrifuged for 5 min at 2000 rpm. Pellets were lysed in ice-cold lysis buffer (1 mM

EDTA, pH 8.0), 10 mM Hepes, 50 mM NaCl, 0.5% Triton X-100, 1 mM phenylmethylsulfonyl fluoride, 5 μM leupeptin, and 10 μg/ml aprotinin). After centrifugation at 8000 rpm for 10 min at 4 °C, supernatants were collected and stored at −20 °C. Crude protein concentrations were determined as described above. For each antibody (OPN and BSP), equal amounts of protein (10 μg/lane) were subjected to SDS–PAGE on 12% polyacrylamide gels. The proteins were then electrophoretically transferred onto Immobilon-P (PVDF) nitrocellulose membranes (Millipore, Bedford, MA). Membranes were blocked with 5% skim milk for 1 h and then incubated with 1:300 diluted rabbit polyclonal antiserum to human OPN (LF-123) and human BSP (LF-100) for 1 h at room temperature. After washing, membranes were incubated with 1:1000 diluted horseradish peroxidase-conjugated-goat-anti rabbit IgG secondary antibody for 1 h, washed with PBS and developed with diaminobenzidine. Blots were scanned and analyzed with a Kodak Electrophoresis Documentation and Analysis System (EDAS) 290. The relative level of each protein was assessed by measuring the integrated intensity of all pixels in each band, excluding the local background. Results are expressed as percentages of protein intensity obtained in control cultures.

### 2.8. Atomic force microscopy

Atomic force microscopy (AFM) was used to determine the morphology and homogeneity of the mineral-like tissue deposited by cementoblastoma-derived cells in the presence of 5 μg/ml normal rabbit IgG antibody (5 μg/ml) or anti-CP antibody (5 μg/ml). AFM (Park Scientific Instruments) was used with an AutoProbe in contact mode with a constant applied force (10 nN) at 1 Hz scan rate in wet samples. Cementoblastoma-derived cells were plated at $2 \times 10^4$ in 24-well culture plates (Costar, Cambridge, MA, USA) onto silicon (1 1 1) monocrystal substrate and cultured for 5 and 15 days in DMEM supplemented with 10% FBS, antibiotics, 50 μg/ml ascorbic acid, 10 mM β-glycerophosphate, and $10^{-7}$ M dexamethasone. Experimental and control cultures were treated every other day with fresh medium and fresh antibody. The cultures were monitored at 5 and 15 days to detect calcium salts precipitation by using Alizarin red S staining. Upon termination of the culture times, cementoblastoma-derived cells were rinsed thrice with ice-cold PBS and culture plates were fixed in situ with 70% ethyl alcohol and air-dried.

### 2.9. Energy dispersive X-ray microanalysis

The composition of the mineral-like tissue formed by the cementoblastoma-derived cells plated onto silicon (1 1 1) monocrystal substrate at an initial density of $2 \times 10^4$ in 24-well plates was analyzed at 5 and 15 days. Control and experimental cultures were maintained in DMEM supplemented as described. Upon termination, the cultures were washed with PBS, fixed in 70% ethyl alcohol, air-dried and covered with a thin gold film, 100 nm thick, to avoid electron disturbances that could interfere with the microanalysis. Cell cultures were analyzed by using a Leica-Cambridge 440 scanning electron microscope fitted with a Pentafet energy dispersive X-ray microanalysis microprobe. All analyses were performed at 20 kV for 300 s (Cuisinier et al., 1991; van Dijk et al., 1995) on different areas with different probe sizes.

### 2.10. Electron diffraction analysis

Human cementoblastoma-derived cells, control and experimental cultures treated as described during 15 days, were tested for mineral phase formation. To do this, cells were cultured on cooper grids of 200 mesh covered with a plastic film and coated with a carbon thin film for TEM observation. D-spacing of diffraction patterns was calibrated to correspond to those for the gold standard obtained with identical diffraction conditions The mineral phase was analyzed using a Jeol 100 CX analytical transmission microscope. All analyses were performed at 100 kV. A Jeol 4000 EX TEM was used at 400 kV for the high-resolution (HRTEM) analysis of the experimental and control cultures at 15 days.

### 2.11. Statistical analysis

Data for the proliferation and viable cell number assays were evaluated by variance analysis followed by multiple comparisons using a corrected Bonferroni $p$ value. Statistics for all other assays were performed with the Student's $t$ test, using Sigma Stat V 2.0 software (Jandel Scientific).

## 3. Results

### 3.1. Cell proliferation and cell viability

To determine whether IgG and anti-CP antibodies contributed to alter human cementoblastoma cells, their proliferation rate was determined during a 10-day period. There were no statistical differences between treatments and 10% FBS-treated controls (Fig. 1A). Cell viability was not affected by either IgG or anti-CP antibodies over the 10-day period as illustrated in Fig. 1B. MTT activity of cementoblastoma cells began to increase on day 3 and continued until day 10. No statistical significances in MTT activity were seen between IgG and anti-CP antibodies with respect to 10% FBS control medium.

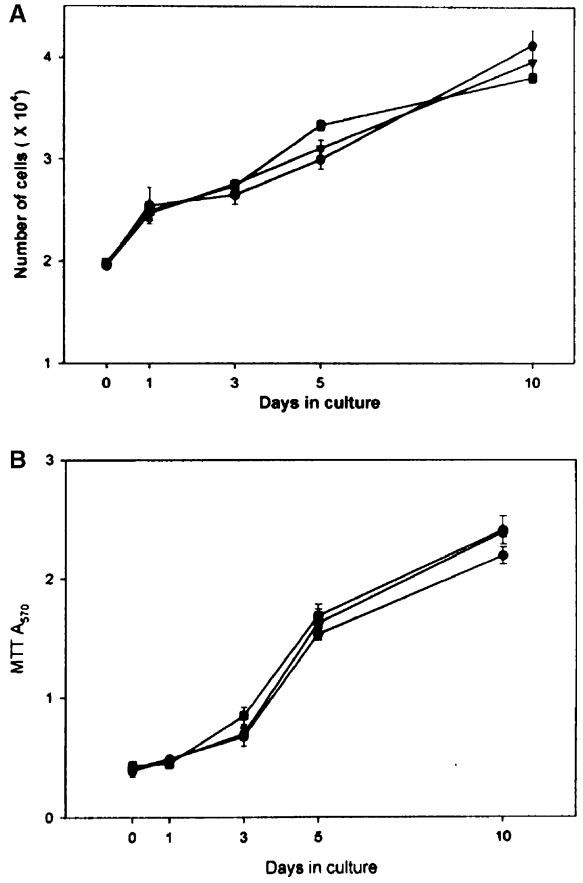


Fig. 1. Effects of IgG, anti-CP antibodies and 10% FBS on cell growth and cell viability. Shown are pooled data from two independent growth curves (A) and from two independent viability curves (B) of cementoblastoma-derived cells treated with IgG (●) and anti-CP antibodies (■), at a concentration of 5 μg/ml each. Ten percent FBS was used as a control media (▼). There were no statistical differences between treatments.

### 3.2. Alkaline phosphatase activity

ALP activity was assessed at different culture times by measuring the enzymatic activity in the cell layer. ALP activity was detected in the cell layers of experimental and control cultures as early as 72 h. No statistical differences between treatments were observed at days 3 and 7. However, alkaline phosphatase activity of cementoblastoma-derived cell cultures treated with anti-CP was 40% ($p < 0.005$), 44% ($p < 0.001$), 49% ($p < 0.1$), and 45% ($p < 0.02$) lower than their counterparts treated with normal rabbit IgG antibody at 9, 11, 13, and 15 days, respectively. These results show that anti-CP antibody inhibited ALP enzymatic activity during the initial stages of mineralization (Fig. 2).

### 3.3. Effect of anti-CP treatment on in vitro expression of OPN and BSP

Analysis of OPN expression reveals that the number of OPN positive cells was lower in the experimental

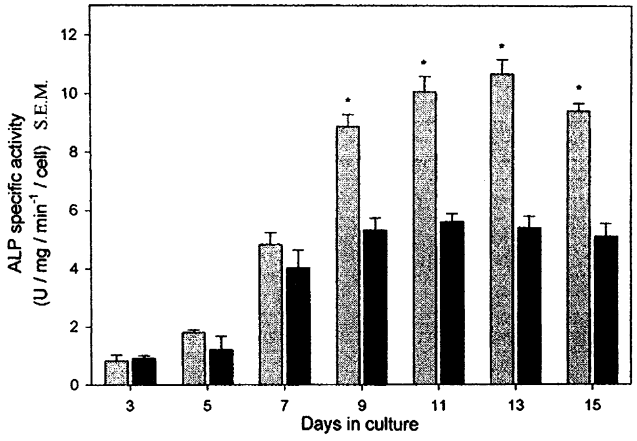


Fig. 2. Alkaline phosphatase activity of human cementoblastoma-derived cells taken at 3, 5, 7, 9, 11, 13, and 15 days. Control cultures (▨) treated with 5 μg/ml of IgG antibody and experimental cultures (■), treated with 5 μg/ml of anti-CP antibody. An asterisk indicates statistical difference between treatments at $p < 0.05$.

cultures by 87, 83, 69, and 52% at 5, 7, 9, and 11 days, than their control counterparts (Fig. 3A and Table 1). However, at 13 and 15 days the values of OPN positive cells in the experimental cultures were similar to those observed in control cultures.

BSP expression was decreased in the cultures treated with anti-CP antibody throughout the entire culture period as compared to controls. BSP positive cell percentages were 82, 51, 60, 80, 83, and 87% lower in experimental cultures than in the control ones at 5, 7, 9, 11, 13, and 15 days (Fig. 3B, Table 2). In the control cultures, a gradual increase in the percentage of BSP positive cells was observed throughout the experimental period. In the experimental cultures the number of BSP positive cells increased 3-fold between days 5–7 and after day 9 decreased gradually to the initial level of day 5.

### 3.4. Immunoblotting

Western analysis showed that, in the experimental cultures, the relative levels of OPN were reduced by 60, 58, 30, 57, 56, and 39% at 5, 7, 9, 11, 13, and 15 days of culture as compared to controls. These results indicate that OPN protein expression was highly inhibited during early stages of the mineralization process (Fig. 4A). BSP relative levels of experimental cultures as compared to control cultures were 30, 18, 50, 16, 17, and 42% at 5, 7, 9, 11, 13, and 15 days, respectively, indicating that anti-CP antibody influenced BSP protein levels at mid and late stages of mineralization (Fig. 4B).

### 3.5. AFM

AFM images showed a sequence of the three-dimensional morphological disposition of the mineral-like

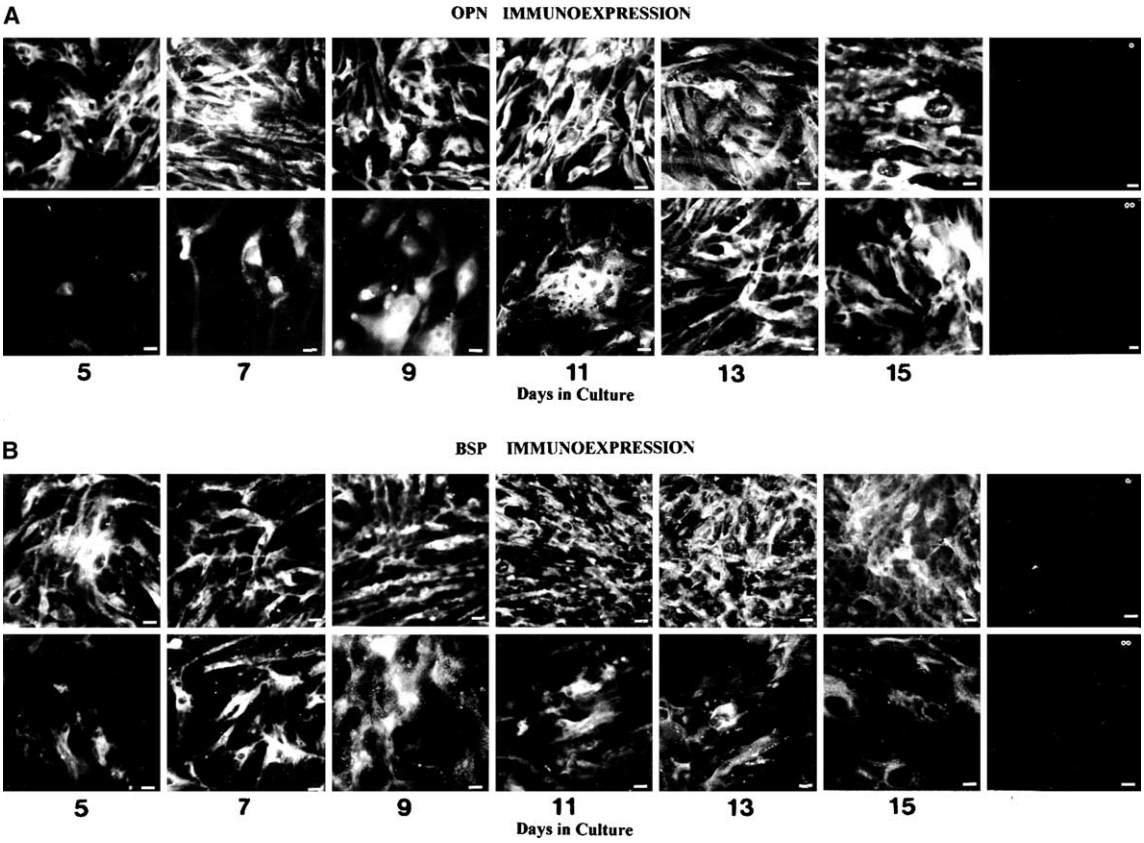


Fig. 3. Immunostaining of cementoblastoma-derived cells with rabbit anti-human OPN polyclonal antibody (A). Experimental cultures treated with 5 μg/ml of anti-CP antibody (lower row) revealed that the number of OPN positive cells was lower by 87, 83, 69, and 52% at 5, 7, 9, and 11 days, than their control counterparts at 5, 7, 9, 11, 13, and 15 days (upper row). Representative negative control with pre-immune rabbit serum for control (°) and experimental (°°) cultures. Original magnification 20×. Bar = 12 μm. Immunostaining of cementoblastoma-derived cells with rabbit anti-human BSP polyclonal antibody (B). Experimental cultures (lower row) treated with 5 μg/ml of anti-CP antibody at 5, 7, 9, 11, 13, and 15 days revealed that BSP expression was dramatically decreased throughout the entire culture period as compared to the control cultures (upper row). Representative negative control with pre-immune rabbit serum for control (°) and experimental (°°) cultures. Original magnification 20×. Bar = 12 μm.

Table 1
Expression of OPN in cementoblastoma-derived cells treated with anti-CP antibody

| Days | Control cultures[a,d] | Experimental cultures[b,d] | %[c] |
|---|---|---|---|
| 5 | 55.4 ± 1.14* | 7.2 ± 0.83 | 13.0 |
| 7 | 62.8 ± 2.16* | 10.4 ± 1.34 | 16.6 |
| 9 | 65.2 ± 2.16* | 20.2 ± 1.30 | 31.0 |
| 11 | 66.2 ± 1.30* | 31.2 ± 2.58 | 47.2 |
| 13 | 70.8 ± 2.16* | 67.4 ± 1.14 | 95.2 |
| 15 | 71.6 ± 1.81 | 69.6 ± 1.14 | 97.3 |

[a] Cementoblastoma-derived cells treated with 5 μg/ml of normal rabbit IgG antibody.
[b] Cementoblastoma-derived cells treated with 5 μg/ml of anti-CP antibody.
[c] Represents percentages of experimental positive cells respect to control cultures.
[d] Means ± SE of triplicates.
* $p < 0.001$ Student's $t$ test.

Table 2
Expression of BSP in cementoblastoma-derived cells treated with anti-CP antibody

| Days | Control cultures[a,d] | Experimental cultures[b,d] | %[c] |
|---|---|---|---|
| 5 | 47.4 ± 2.40* | 8.40 ± 0.89 | 17.8 |
| 7 | 54.2 ± 1.48* | 26.4 ± 2.07 | 48.8 |
| 9 | 55.2 ± 1.09* | 22.0 ± 1.58 | 39.8 |
| 11 | 68.8 ± 0.83* | 13.4 ± 1.14 | 19.5 |
| 13 | 76.4 ± 1.14* | 12.4 ± 1.34 | 16.7 |
| 15 | 79.8 ± 1.48* | 9.8 ± 1.64 | 12.3 |

[a] Cementoblastoma-derived cells treated with 5 μg/ml of normal rabbit IgG antibody.
[b] Cementoblastoma-derived cells treated with 5 μg/ml of anti-CP antibody.
[c] Represents percentages of experimental positive cells respect to control cultures.
[d] Means ± SE of triplicates.
* $p < 0.001$ Student's $t$ test.

tissue deposited by cementoblastoma cells. The features observed in control cultures, at 5 days, revealed granular agglomerates with a size range of 1.5–0.30 μm and grain agglomeration that favored the formation of crystalline plaques with a lamellar-like pattern. These individual plaques were 0.18 μm wide and 0.36 μm

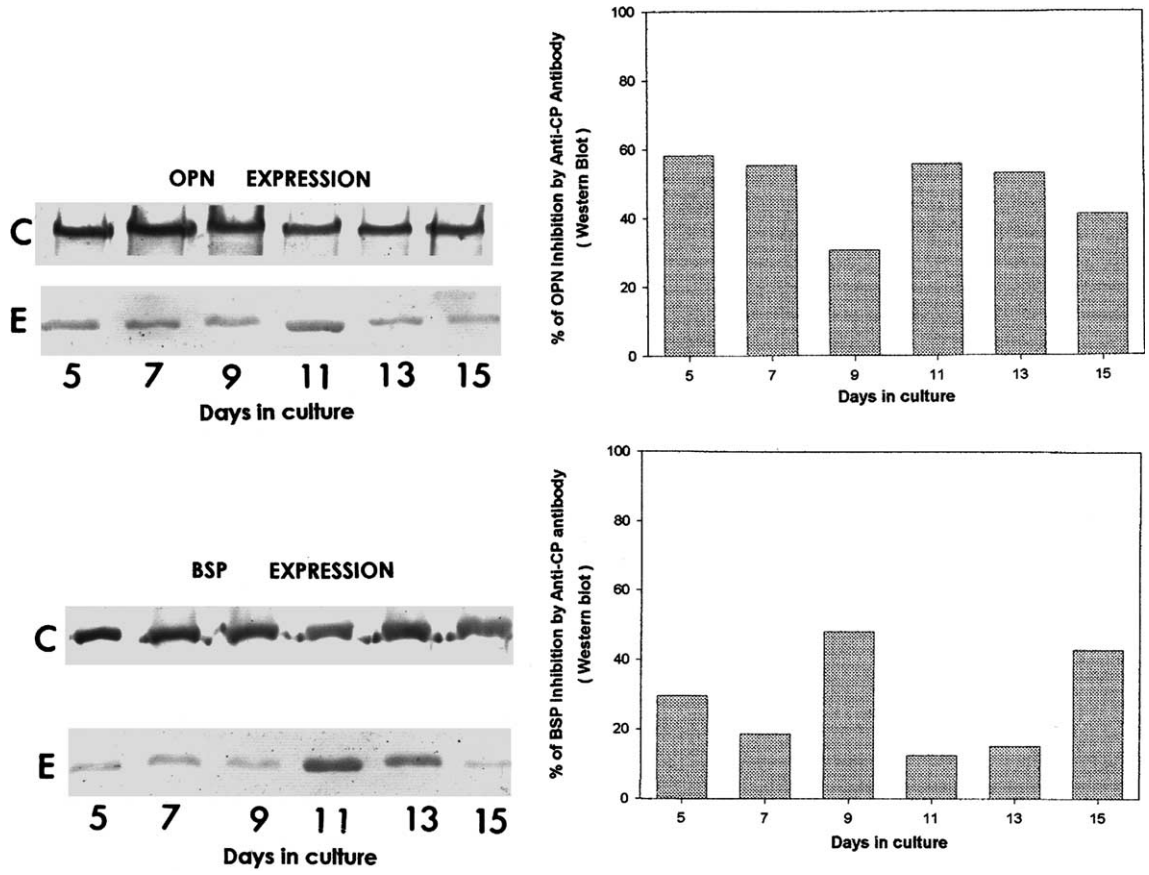


Fig. 4. Western blots for the detection of OPN and BSP in cementoblastoma-derived cells treated with IgG antibodies (C) and with anti-CP antibodies (E). Solubilized extracts from different culture times (5–15 days) were subjected to SDS–PAGE and then to immunodetection with antibodies to human OPN and BSP. Protein relative levels were assessed by measuring the integrated intensity of all pixels in each band, excluding the local background.

long, representing an anisotropic crystalline structure of 2:1 (l/w); with small granular particles (0.3 μm, and 300 Å high), (Fig. 5A). Tiny needle-shaped crystals 6 Å high with preferential orientation were observed (Fig. 5E). Experimental cultures treated during 5 days with anti-CP antibody showed a tiny granular morphology with a submicron size (0.1 μm) of granular particles that formed the agglomerates with a size range of 1.3–0.25 μm (Fig. 5B) and spherical agglomerates (Fig. 5F). Control cultures at 15 days showed well-oriented and organized plaque-like structures of 1.6 μm width and 20 μm length, representing an anisotropic ratio of 12.5 (l/w). These cultures also showed granular agglomerates with a size range of 2.6–0.9 μm. (Fig. 5C) and needle-shaped crystals (Fig. 5G). Experimental cultures at 15 days revealed almost the same features observed in experimental cultures at 5 days. The agglomerates maintained spherical morphology without organization of needle-like crystals to form plaque-like structures. However, the granular agglomerates were larger in size (1.5–0.30 μm), when compared to those observed at 5 days of experimental cultures (Figs. 5D and H)).

### 3.6. EDS

The Ca/P ratio and composition of the mineral-like tissue deposited in vitro by cementoblastoma-derived cells was assessed at 5 and 15 days of culture. Control cultures at 5 days showed 56.1 and 38.7 at.% of $Ca^{2+}$ and P, respectively (Fig. 6C). Other elements such as K (2.5 at.%), and $Mg^{2+}$ (2.4 at.%) were present in their global composition. The Ca/P ratio (1.45) corresponds well with the biological hydroxyapatite value (Fang et al., 1994). Cementoblastoma cell cultures treated with 5 μg/ml of anti-CP antibody for 5 days showed low energy peaks for $Ca^{2+}$ and P (Fig. 6A) with an atomic percentage of 29.9 and 58.5, respectively. Other elements such as K represented 5.4 of the atomic percentage. $Mg^{2+}$ ions were not detectable in the spectrum. The Ca/P ratio value was of 0.50. At 15 days of culture, control cultures exhibited 55.4 and 34.4 at.% for $Ca^{2+}$ and P (Fig. 6D). K and $Mg^{2+}$ were present in the composition with 6.1 and 3.8 at.%. The Ca/P ratio was 1.61, which corresponds well with the biological hydroxyapatite value. Experimental cultures revealed 38.5, 48.3, and 4.5 at.% for $Ca^{2+}$, P, and K (Fig. 6B). The Ca/P ratio

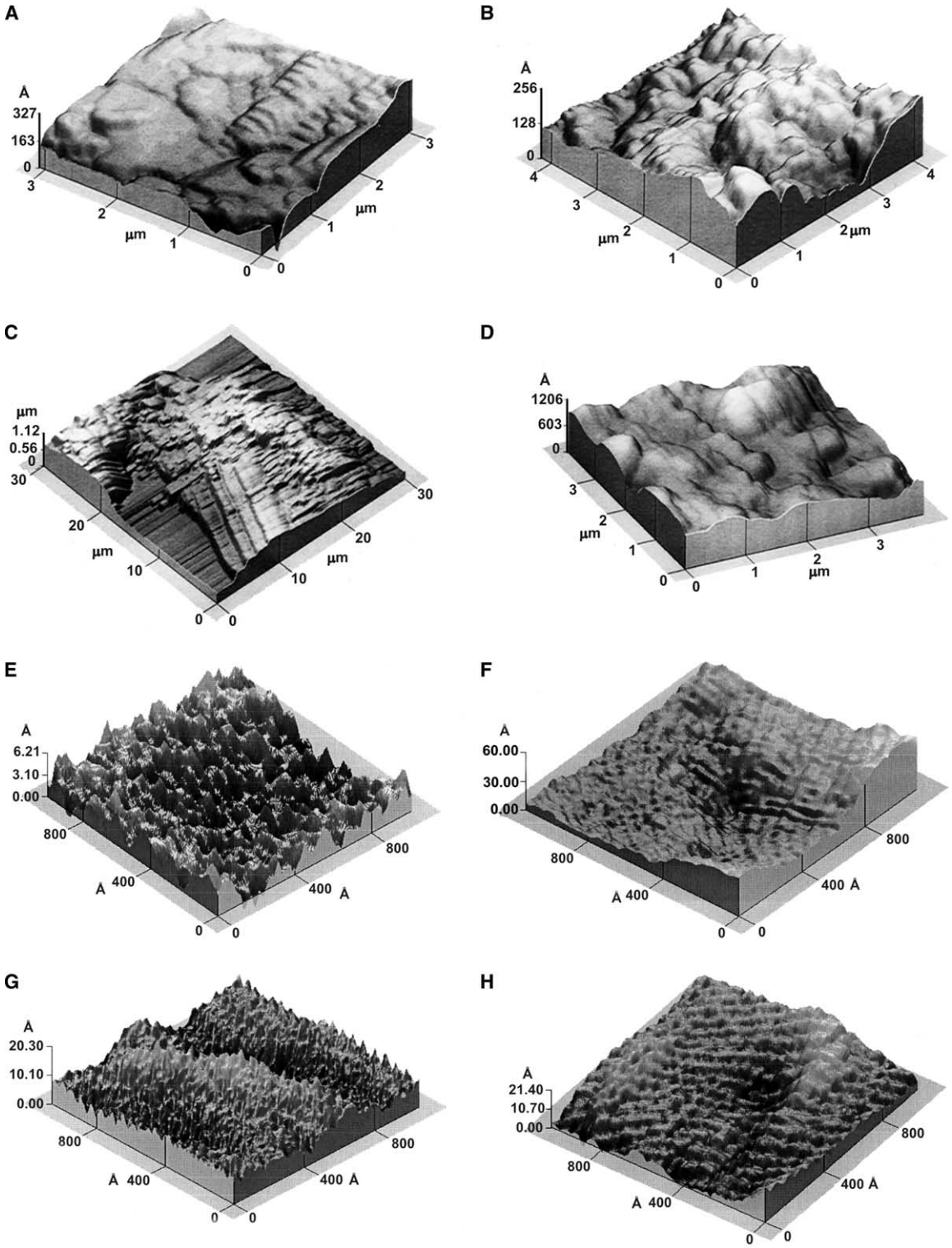


Fig. 5. Three-dimensional features observed by AFM showed globular, needle-shaped crystals and lamellar arrangement of the mineralized-like tissue deposited by cementoblastoma-derived cells in control cultures at 5 days (A and E), and 15 days of culture (C and G). Experimental cultures treated with 5 µg/ml of anti-CP antibody revealed similar spatial disposition of globular-like structures at 5 days (B and F), and 15 days of culture without lamellar arrangement of the mineralized-like tissue deposited by cementoblastoma-derived cells (D and H).

was 0.79. Energy dispersive X-ray microanalysis (EDS) examination determined the biological hydroxyapatite values. Therefore, the EDS spectra from control samples showed better peak definition than those of the experimental cultures which reveals that the crystal density was larger in the control cultures.

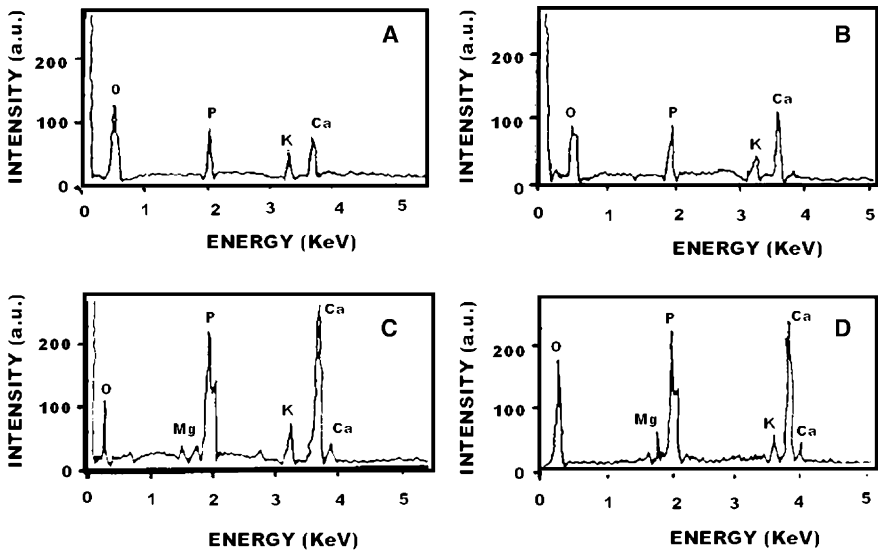


Fig. 6. Representative energy-dispersive x-ray microanalysis spectrum of a $1 \times 1$ mm area of mineralized areas deposited by putative human cementoblasts. Experimental cultures at 5 (A) and 15 (B) days showed low peaks for calcium ($Ca^{2+}$) and phosphorous (P). Control cultures showed prominent peaks of $Ca^{2+}$ and P and peaks representing $Mg^{2+}$ and K at 5 (C) and 15 (D) days of culture.

### 3.7. Electron diffraction

Cell cultures from cementoblastoma-derived cells were obtained for the analysis of mineral deposits at 15 days of culture. Control and experimental cultures showed crystals that revealed patterns of concentric double rings. The inner double rings correspond to D-spacing, 2.34 and 2.98 Å (Figs. 7A and B, respectively), which were consistent with those for hydroxyapatite (2.29 and 3.08 Å). The inner semi-ring in Fig. 7 shows a clear preferential growth of hydroxyapatite crystals.

Examination of the crystallinity of samples with HRTEM showed that both control and experimental cultures at 15 days revealed a homogeneous and preferential spatial arrangement of hydroxyapatite crystallites with a 7.1 Å (h k l: 1 0 0), 3.8 Å (h k l: 1 1 1), and 3.1 Å (h k l: 2 1 0) interatomic distances (Fig. 8). All the crystals were nanostructured with atomic distances of hydroxyapatite crystals values of *d*: 2.27 Å (h k l: 2 1 2), 2.42 Å (h k l: 3 0 1), 3.53 Å (h k l: 2 0 1) and 4.5 Å (h k l: 1 1 0). The patterns obtained are shown in Fig. 7 and were indexed with the hydroxyapatite standard patterns of the JCPDS (Joint Committee on Powder Standards) No. 9-432 file for calcium hydroxyapatite (JCPDS, 1995).

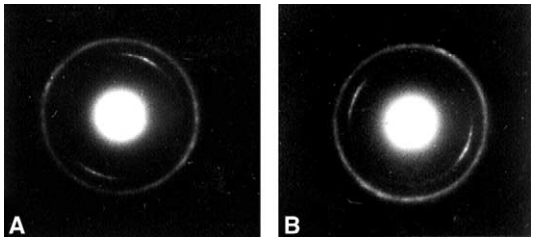


Fig. 7. Selected area electron diffraction pattern obtained from mineralized-like tissue deposited by cementoblastoma-derived cells. The inner semi-ring shows a clear preferential growth of hydroxyapatite crystals at 15 days for both, control (A) and experimental (B) cultures.

### 3.8. Scanning electron microscopy

Examination of control cultures at 5 days revealed mineralized areas formed by agglomerates and needle-like structures (Fig. 9C), confirming the electron diffraction analysis and AFM images. At 15 days, control cultures formed plaque-like structures (Fig. 9D). However, experimental cultures at 5 and 15 days showed agglomerates with spherical shape and homogeneous size. (Figs. 9A and B, respectively). It was evident that in the cultures treated with anti-CP antibody the growth of the mineralized area was retarded.

## 4. Discussion

The results of this study indicate that mineralization in a cementoblastic cell line was partially inhibited by anti-CP, indicating that the CP is among the factors that regulate mineral deposition of this lineage in vitro. Anti-CP antibody influenced the ALP activity and the protein levels of OPN and BSP as well as the amount and quality of mineral deposited in these cultures without interfering with cell proliferation and cell viability. Cell viability was greater than 90% for all treatment groups, eliminating the likelihood of cell toxicity caused by either IgG or anti-CP antibodies The dosages of IgG and anti-CP antibodies were similar to those used for in vitro studies reported by Shakibaei, 1998). ALP activity,

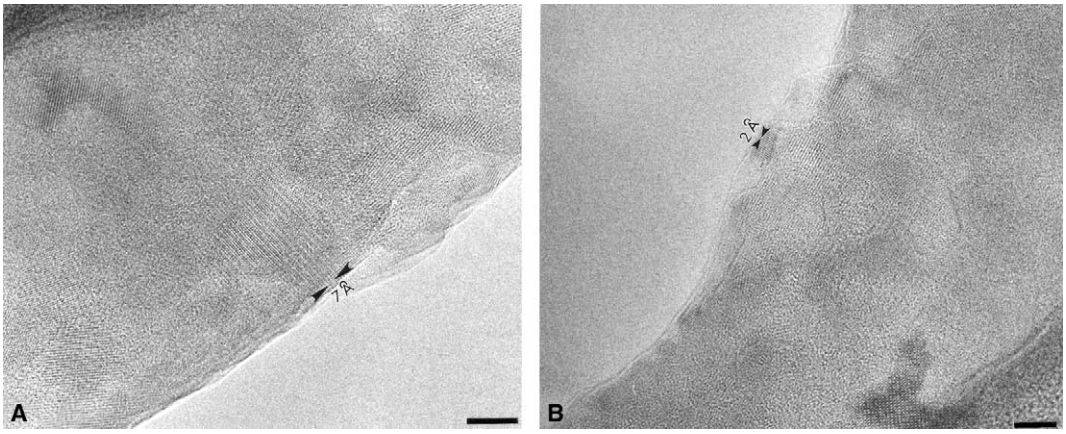


Fig. 8. High-resolution transmission electron microscopy (HRTEM) shows that crystallinity of the mineralized-like tissue in control cultures at 15 days was homogeneous and with a preferential spatial arrangement of hydroxyapatite crystallites (A). Experimental cultures at 15 days showed non-homogeneous hydroxyapatite crystallite arrangement (B). Bar in A = 1.7 nm. Bar in B = 1.4 nm.

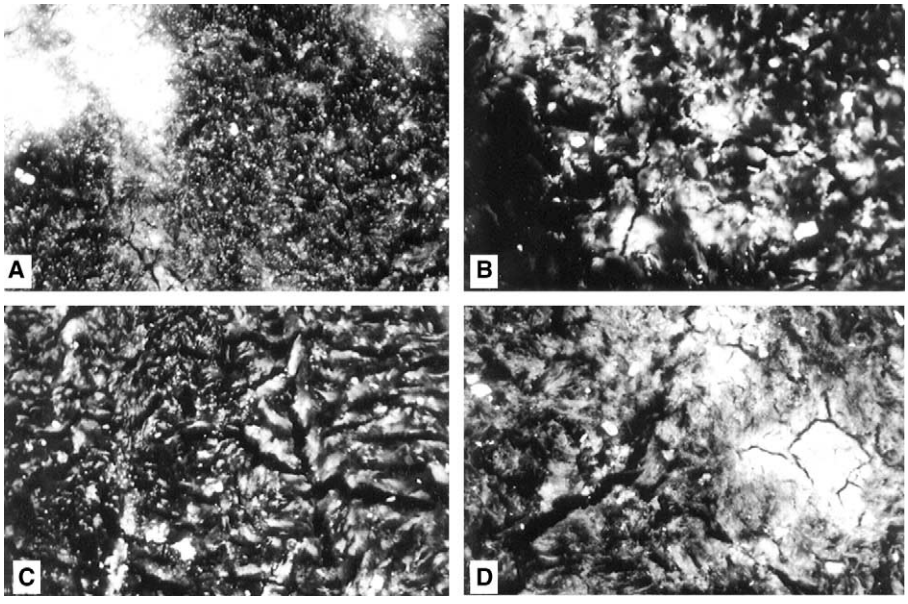


Fig. 9. SEM examination of the mineral-like tissue deposited by cementoblastoma-derived cells revealed agglomerate and needle-like structures at 5 (A) and 15 (B) days. Experimental cultures at 5 (C) and 15 (D) days show agglomerates with spherical shape and homogeneous size. Bar = 30 μm.

expression of OPN and BSP are characteristic of early and late stages of mineral-like tissue deposition in osteoblastic and cementoblastic cell lines in vitro. Since the cementoblastic cell line used in this study has been shown to express CAP, which is immunologically related to CP (Arzate et al., 2002), and CAP has also been reported as a 65 kDa species in developing tooth germ (Saito et al., 2001), it is possible that CP represents a CAP-related molecular form. In addition anti-CP antibody has the capacity to identify putative cementoblastic populations both in vitro and in vivo.

ALP is thought to play a role in general phosphate metabolism and cementum formation, although its precise role during mineralization is not entirely clear (Linde, 1982). ALP activity is related to the initial mineralization and once the phase of bulk matrix synthesis and mineralization has ceased, the further progression of mineralization of previously deposited matrix is associated with retention of ALP activity (Bianco, 1992). Our experimental cultures revealed an up to 49% decrease in ALP activity from 9 to 15 days, suggesting that anti-CP antibody partially inhibited ALP activity during mineralization in the experimental cultures. In addition to this, the thickness of the cementum-like tissue deposited by cementoblastoma-derived cells in the experimental cultures, as analyzed by AFM, was thinner than that observed in control cultures. The present results support previous work where a highly

significant positive correlation between ALP activity and cementum thickness has been demonstrated, i.e., the higher the activity of the enzyme, the thicker the cementum layer. Besides inhibition of ALP activity causes severe inhibition of cementum formation. Thus, ALP appears to be essential for the continuous growth of cementum (Beertsen et al., 1999; Groeneveld et al., 1995; Vandenbos and Beertsen, 1999). These results provide further support to our previous data, which point to the capability of CP to promote mineralization in undifferentiated mesenchymal cells (Arzate et al., 1996) and ALP activity in cementoblastoma cells (Arzate et al., 1998).

It has been suggested that non-collagenous proteins, such as OPN and BSP, have a major role in filling spaces created during collagen assembly, imparting cohesion to the mineral-like tissue by allowing mineral deposition to spread across the entire collagen meshwork (Bosshardt et al., 1998; Nanci, 1999). However, the means by which mineralization is achieved is still not well understood. Several authors suggest that phosphoproteins such as BSP and OPN are necessary for the initiation of crystal formation (Roach, 1994), and the large highly ordered fibrils of type I collagen. The major phosphoproteins in cementum are OPN and BSP and are synthesized by cementoblasts (Chen et al., 1991b; MacNeil et al., 1998; Shapiro et al., 1993). Our results revealed that OPN at the protein level was highly depressed in the experimental cultures during the initial stages of mineralization and the highest effect on BSP protein levels was observed at the mid and late stages of the experimental period as revealed by immunocytochemistry and Western blots. Since OPN is expressed at high levels in mineralized connective tissues (Bianco et al., 1991) and is related to the initial growth of hydroxyapatite crystals, it seems that the anti-CP antibody could have a secondary effect during initiation and progression of the mineralized matrix. Our results suggest that CP could mediate initial stages of mineralization probably by influencing OPN availability during crystal growth and maturation. Since, OPN's ability to bind and potentially orient significant amounts of $Ca^{2+}$ which suggests that might function to promote calcification (Butler et al., 1996; Gorski, 1992). However, OPN is a multifunctional protein and indeed, in vitro studies support a role for OPN as an inhibitor of calcium oxalate crystals in the kidney and in cell-free systems, and acts principally on crystal growth (Hunter et al., 1996). It has been reported that OPN is abundant at sites of calcification in human atheroschlerotic plaques and in calcified aortic valves, but is not found in normal arteries (Butler et al., 1996). However the function of OPN in hard tissue formation, mineralization and turnover is not yet clear, and the mineral inhibition during the mineralization process cannot be attributable to OPN acting solely as an inhibitor of crystal growth without considering the possible role of ALP on OPN's dephosphorylation, since phosphorylation of OPN is required for its inhibitory effect in an in vitro mineralization system (Jono et al., 2000). BSP plays an important role in mineral nucleation (Chen et al., 1991a, 1992b). BSP has a precise spatial association with early mineral aggregates, binds strongly to hydroxyapatite and acts as a specific and potent nucleator for hydroxyapatite formation in vitro (Hunter and Goldberg, 1993). Our findings demonstrate that BSP protein levels were partially depressed throughout the entire culture time. Thus, the process of mineral nucleation and growth was probably partially inhibited in the experimental cultures by affecting availability of OPN and ALP to regulate calcium uptake (Fukayama and Tashijan, 1990), crystal growth and maturation, and BSP crystal nucleation, explaining the globular mineral aggregates that did not develop to form lamellar structures in these cultures.

This statement is supported by the compositional data of the mineralized-like tissue deposited by cementoblastoma-derived cell cultures at 5 and 15 days as observed in the experimental cultures, since Ca/P ratio was lower when compared to controls and is related to a lesser crystal density. It appears that the calcium uptake deposition was retarded, since experimental cultures presented lower values of $Ca^{2+}$ than control cultures at 5 and 15 days This result could be related to the partial inhibition of OPN protein levels and ALP activity. It has been shown that other elements such as potassium and small concentrations of ions, like $Mg^{2+}$, slow crystal development by adsorbing to and blocking surface growth sites and hydroxyapatite crystal formation and maturation (Amjad et al., 1984; Serre et al., 1998; Weismann et al., 1997). $Mg^{2+}$ ions are not directly incorporated into the apatite structure, but are rather accumulated in the hydration shell around the hydroxyapatite crystal, forming surface-bound ionic complexes (Posner, 1969). Our results revealed that magnesium was absent in the experimental cultures, which could contribute to the crystal growth retardation observed at 15 days of culture in cells treated with the anti-CP antibody. However, relatively high potassium concentrations and accumulation might be a common feature of mineralizing matrices. EDS examination of the mineralized-like tissue revealed that the material deposited by cementoblastoma-derived cells represents hydroxyapatite in both, control and experimental cultures at 15 days.

This is also supported by the analysis of HRTEM images. However, experimental cultures at 15 days had smaller crystallites in the range of nanocrystals and both control and experimental cultures have a preferential crystallographic orientation. This occurs within a matrix characterized by the lack of orientation of collagen fibrils in coherent directions and is characterized by the initial formation of randomly distributed, roughly

spherical, aggregates of crystals radiating from a center. In contrast, the control cultures showed the ordered mineralization pattern of lamellar-like mineralized tissue, matching a significant degree of collagen spatial organization and orientation (Boyde and Hobdell, 1969). Recent findings suggest that growth layers in human cementum may be related to altered mineral crystal orientation (Cool et al., 2002). Our observations strengthen the argument that mineral crystals are responsible for the layers observed in cementoblastoma control cultures and that the anti-CP antibody and the decreased ALP activity could contribute to the partial inhibition during the development of this morphological pattern and mineral crystal alignment (Tesch et al., 2003), presumably as a result of crystal density and impaired mineral maturation as revealed by EDS and HRTEM examination of the mineral phase in the experimental cultures.

Finally, our observations and combined data analysis suggest a provocative role of CP during the biological mineralization process of cementum-like tissue in vitro. Consistent with this idea, are the partial inhibition of ALP activity, decreased protein levels of OPN and BSP, compositional, morphological changes, and the retardation of the mineral phase by human putative cementoblastic cells, observed during the development of mineralized matrix. However, further studies are necessary to show the biological significance of CP among the factors that regulate cementum extracellular matrix mineralization in vitro, since its specific role cannot be determined conclusive at this time.

## Acknowledgments

The authors wish to thank Dr. Larry W. Fisher for the gift of polyclonal antibodies against OPN (LF-123) and BSP (LF-100). Rogelio Fragoso from CINVESTAV-México, José Guzmán from IIM-UNAM, Luis Rendón, Pedro Mexía, Carlos Flores, and Roberto Hernández from IF-UNAM, for their technical assistance during the course of this study. Their support is greatly appreciated. This research was partially supported by DGAPA-UNAM (IN200599, IN200501) and CONACyT 30735-M.

## References

Amjad, Z., Koutsoukos, P.G., Nancollas, G.H., 1984. The crystallization of hydroxyapatite and fluoroapatite in the presence of magnesium ions. J. Colloid Interface Sci. 101, 250–256.

Arzate, H., Olson, S.W., Page, R.C., Gown, A.M., Narayanan, A.S., 1992. Production of a monoclonal antibody to an attachment protein derived from human cementum. FASEB J. 6, 2990–2995.

Arzate, H., Chimal-Monroy, J., Hernández-lagunas, L., Díaz de León, L., 1996. Human cementum protein extract promotes chondrogenesis and mineralization in mesenchymal cells. J. Periodont. Res. 31, 144–148.

Arzate, H., Alvarez-Pérez, M.A., Aguilar-Mendoza, M.E., Alvarez-Fregoso, O., 1998. Human cementum tumor cells have different features from human osteoblastic cells in vitro. J. Periodont. Res. 33, 249–258.

Arzate, H., Alvarez-Pérez, M.A., Alvarez-Fregoso, O., Wusterhaus-Chávez, A., Reyes-Gasga, J., Ximénez-Fyvie, L.A., 2000. Electron microscopy, micro-analysis and X-ray diffraction characterization of the mineral-like tissue deposited by human cementum tumor-derived cells. J. Dent. Res. 79, 28–34.

Arzate, H., Jiménez-García, L.F., Alvarez-Pérez, M.A., Landa, A., Bar-Kana, I., Pitaru, S., 2002. Immunolocalization of a human cementoblastoma conditioned medium-derived protein. J. Dent. Res. 81, 541–546.

Bar-Kana, I., Narayanan, A.S., Savion, N., Pitaru, S., 1999. Cementum attachment protein enriches the cementoblastic population on root surfaces in vitro. J. Dent. Res. 78, 213 (special Issue Abstr # 857).

Beertsen, W., van den Bos, T., Everts, V., 1999. Root development in mice lacking functional tissue non-specific alkaline phosphatase gene: inhibition of acellular cementum formation. J. Dent. Res. 78, 1221–1229.

Bianco, P., Fisher, L.W., Young, M.F., Termine, J.D., Robey, P.G., 1991. Expression of bone sialoprotein (BSP) in developing human tissues. Calcif. Tissue Int. 49, 421–426.

Bianco, P., 1992. Structure and mineralization of bone. In: Bonucci, E. (Ed.), Calcification in Biological Systems. CRC Press, Boca Raton, FL, pp. 244–268.

Bosshardt, D.D., Zalzal, S., McKee, M.D., Nanci, A., 1998. Developmental appearance and distribution of bone sialoprotein and osteopontin in human and rat cementum. Anat. Rec. 250, 13–33.

Boskey, A.L., 1995. Osteopontin and related phosphorylated sialoproteins: effects on mineralization. Ann. N.Y. Acad. Sci. 760, 249–256.

Boyde, A., Hobdell, M.H., 1969. Scanning electron microscopy of lamellar bone. Z. Zelforsch. Mikrosk. Anat. 93, 213–231.

Bradford, M.M., 1976. A rapid and sensitive method for the quantitation of microgram quantities of protein utilizing the principle of protein-dye binding. Ann. Biochem. 72, 248–254.

Bronckers, A.L., Farach-Carson, M.C., Van Waveren, E., Butler, W.T., 1994. Immunolocalization of osteopontin, osteocalcin, and dentin sialoprotein during dental root formation and early cementogenesis in the rat. J. Bone Miner. Res. 9, 833–841.

Butler, W.T., Ridall, A.L., McKee, M.D., 1996. Osteopontin. In: Bilezikian, J.P., Raisz, L.G., Rodan, G.A. (Eds.), Principles of Bone Biology. Academic Press, San Diego, CA, pp. 167–181.

Chen, J.K., Shapiro, H.S., Wrana, J.L., Reimers, S., Heersche, J.N., Sodek, J., 1991a. Localization of bone sialoprotein (BSP) expression to sites of mineralized tissue formation in fetal rat tissues by in situ hybridization. Matrix 11, 133–143.

Chen, J., Zhang, Q., McCulloch, C.A., Sodek, 1991b. Immunohistochemical localization of bone sialoprotein in foetal porcine bone tissues: comparisons with secreted phosphoprotein I (SSP-I, osteopontin) and SPARC (osteonectin). Histochem. J. 23, 281–289.

Chen, J., Shapiro, H.S., Sodek, J., 1992a. Developmenal expression of bone sialoprotein mRNA in rat mineralized connective tissues. J. Bone Miner. Res. 7, 987–997.

Chen, Y., Bal, B.S., Gorski, J.P., 1992b. Calcium and collagen binding properties of osteopontin, bone sialoprotein, and bone acidic glycoprotein-75 from bone. J. Biol. Chem. 267, 24871–24878.

Cool, S.M., Forwood, M.R., Campbell, P., Bennett, M.B., 2002. Comparisons between bone and cementum compositions and the possible basis for their layered appearances. Bone 30, 386–392.

Cuisinier, M.J., Glaisher, R.W., Voegel, J.C., Hutchinson, J.L., Brès, E.F., Frank, R.M., 1991. Compositional variations in apatites with respect to preferential ionic extraction. Ultramicroscopy 36, 297–305.

D'Errico, J.A., Berry, J.E., Ouyang, H., Strayhorn, C.L., Windle, J.J., Somerman, M.J., 2000. Employing a transgenic animal model to obtain cementoblasts in vitro. J. Periodontol. 71, 63–72.

Dunbar, B.S., Schwoebel, E.D., 1990. Guide to protein purification. Section XI. Immunological procedures. Preparation of polyclonal antibodies. Methods Enzymol. 182, 663–670.

Fang, Y., Agrawal, D.K., Roy, D.M., 1994. Termal stability of synthetic hydroxyapatite. In: Handbook of Bioactive Ceramics, vol. III. CRC Press, Boca Raton, FL, pp. 269–282.

Fukayama, S., Tashijan Jr., A.H., 1990. Stimulation by parathyroid hormone of 45 $Ca^{2+}$ uptake in osteoblast-like cells: possible involvement of alkaline phosphatase. Endocrinology 126, 1941–1949.

Gorski, J., 1992. Acidic phosphoproteins from bone matrix: a structural rationalization of their role in biomineralization. Calcif. Tissue Int. 50, 391–396.

Groeneveld, M.C., Everts, V., Beertsen, W., 1995. Alkaline phosphatase activity in the periodontal ligament and gingiva of the rat molar: its relation to cementum formation. J. Dent. Res. 74, 1374–1381.

Hunter, G.K., Goldberg, H.A., 1993. Nucleation of hydroxyapatite by bone sialoprotein. Proc. Natl. Acad. Sci. USA 90, 8562–8565.

Hunter, G.K., Hauschka, P.V., Poole, R.A., Rosenberg, L.C., Goldberg, H.A., 1996. Nucleation and inhibition of Hydroxyapatite formation by mineralized tissue proteins. Biochem. J. 317, 59–64.

JCPDS, 1995. Joint Committee on Powder Diffraction Standards No. 9-432 file for calcium hydroxyapatite.

Jono, S., Peinado, C., Giachelli, C.M., 2000. Phosphorylation of osteopontin is required for inhibition of vascular smooth muscle cell calcification. J. Biol. Chem. 275, 20197–20203.

Kagayama, M., Li, H.C., Zhu, J., Sasano, Y., Hatakeyama, Y., Mizoguchi, I., 1997. Expression of osteocalcin in cementoblasts forming acellular cementum. J. Periodont. Res. 32, 273–278.

Kramer, I.R.H., Pindborg, J.J., Shear, M., 1992. In: Histological Typing of Odontogenic Tumors. World Health Organization, International Histological Classification of Tumours, second ed. Springer, Berlin, p. 23.

Linde, A., 1982. On enzymes associated with biological calcification. In: Veis, A. (Ed.), The Chemistry and Biology of Mineralized Connective Tissue. Elsevier, New York, pp. 559–570.

Liu, H.W., Yacobi, R., Savion, N., Narayanan, A.S., Pitaru, S., 1997. A collagenous cementum-derived attachment protein is a marker for progenitors of the mineralized tissue-forming cell lineage of the periodontal ligament. J. Bone Miner. Res. 12, 1691.

Lowry, O.H., Roberts, N.R., Wu, M.-L., Hixon, W.S., Crawford, E.J., 1954. The quantitative histochemistry of brain I. Enzyme measurement. J. Biol. Chem. 207, 19–37.

MacNeil, R.L., Berry, J., D'Errico, J., Strayhorn, C., Piotrowski, B., Somerman, M.J., 1995. Role of two mineral-associated adhesion molecules, osteopontin and bone sialoprotein, during cementogenesis. Connect. Tissue Res. 33, 1–7.

MacNeil, R.L., D'Errico, J.A., Ouyang, H., Berry, J., Strayhorn, C., Somerman, M.J., 1998. Isolation of murine cementoblasts: unique cells or uniquely-positioned osteoblasts? Eur. J. Oral Sci. 106 (Suppl. 1), 350–356.

McAllister, B., Narayanan, A.S., Miki, Y., Page, R.C., 1990. Isolation of a fibroblast attachment protein from cementum. J. Periodont. Res. 25, 99–105.

Nanci, A., 1999. Content and distribution of noncollagenous matrix proteins in bone and cementum: relationship to speed of formation and collagen packing density. J. Struct. Biol. 126, 256–269.

Oldberg, A., Franzen, A., Heinegard, D., 1988. The primary structure of a cell-binding bone sialoprotein. J. Biol. Chem. 263, 19430–19432.

Olson, S., Arzate, H., Narayanan, A.S., Page, R.C., 1991. Cell attachment activity of cementum proteins and mechanism of endotoxin inhibition. J. Dent. Res. 70, 1272–1277.

Pitaru, S., Narayanan, A.S., Olson, S., Savion, N., Hekmati, H., Alt, I., Metzger, 1995. Specific cementum attachment protein enhances selectively the attachment and migration of periodonal cells to root surfaces. J. Periodont. Res. 30, 360–368.

Posner, A.S., 1969. Crystal chemistry of bone mineral. Physiol. Rev. 49, 760–792.

Saito, M., Iwase, M., Maslan, S., Nozaki, N., Yamauchi, M., Handa, K., Takahashi, O., Sato, S., Kawase, T., Teranaka, T., Narayanan, A.S., 2001. Expression of cementum-derived attachment protein in bovine tooth germ during cementogenesis. Bone 29, 242–248.

Roach, H.I., 1994. Why does bone matrix contain non-collagenous proteins? The possible roles of osteocalcin, osteonectin, osteopontin and bonesialoprotein in bone mineralization and resorption. Cell Biol. Int. 18, 617–628.

Serre, C.M., Papillard, M., Chavassieux, P., Voegel, J.C., Boivin, G., 1998. Influence of magnesium substitution on collagen-apatite biomaterial on the production of a calcifying matrix by human osteoblasts. J. Biomed. Mater. Res. 42, 626–633.

Shakibaei, M., 1998. Inhibition of chondrogenesis by integrin antibody in vitro. Exp. Cell Res. 240, 95–106.

Shapiro, H.S., Chen, J., Wrana, J.L., Zhang, Q., Blum, M., Sodek, J., 1993. Characterization of porcine bone sialoprotein: primary structure and cellular expression. Matrix 13, 431–440.

Tesch, W., Vandenbos, T., Roschgr, P., Fratzl-Zelman, N., Klaushofer, K., Beertsen, W., Fratzl, P., 2003. Orientation and mineral crystallites and mineral density during skeletal development in mice deficient in tissue nonspecific alkaline phosphatase. J. Bone Miner. Res. 18, 117–125.

Vandenbos, T., Beertsen, W., 1999. Alkaline phosphatase activity in human periodontal ligament: age effect and relation to cementum growth rate. J. Periodont. Res. 34, 1–6.

van Dijk, K., Schaeken, H.G., Marèe, C.H.M., Verhoeven, J., Wolke, J.C.G., Habraken, F.H.P., Jansen, J.A., 1995. Influence of Ar pressure on r.f. magnetron-sputtered $Ca_5(PO_4)_3OH$ layers. Surf. Coat. Technol. 76, 206–210.

Weismann, H.P., Tkotz, T., Joos, U., Zierold, K., Stratmann, U., Szuwart, T., Plate, U., Höhling, H.J., 1997. Magnesium in newly formed dentin mineral of rat incisor. J. Bone Miner. Res. 12, 380–383.

Wu, D., Ikezawa, K., Parker, T., Saito, M., Narayanan, A.S., 1996. Characterization of a collagenous cementum-derived attachment protein. J. Bone Miner. Res. 11, 686–692.